



UNH-05-04
LBNL-57663
MIT-CTP-3653
CALT-68-2564
NT@UW-05-03

$I = 2$ Scattering from Fully-Dynamical Mixed-Action Lattice QCD

Silas R. Beane,^{1,2} Paul F. Bedaque,³ Kostas Orginos,⁴ and Martin J. Savage^{4,5,6}

(NPLQCD Collaboration)

¹Department of Physics, University of New Hampshire, Durham, NH 03824-3568.

²Jefferson Laboratory, 12000 Jefferson Avenue, Newport News, VA 23606.

³Lawrence-Berkeley Laboratory, Berkeley, CA 94720.

⁴Center for Theoretical Physics, MIT, Cambridge, MA 02139.

⁵California Institute of Technology, Pasadena, CA 91125.

⁶Department of Physics, University of Washington, Seattle, WA 98195-1560.

Abstract

We compute the $I = 2$ scattering length at pion masses of $m_\pi = 294, 348$ and 484 MeV in fully-dynamical lattice QCD using Luscher's finite-volume method. The calculation is performed with domain-wall valence-quark propagators on asqtad-improved MILC configurations with staggered sea quarks at a single lattice spacing, $b = 0.125$ fm. Chiral perturbation theory is used to perform the extrapolation of the scattering length from lattice quark masses down to the physical value, and we find $a_2 = 0.0426 \pm 0.0006 \pm 0.0003 \pm 0.0018$, in good agreement with experiment. The $I = 2$ scattering phase shift is calculated to be $\delta = 43 \pm 10^\circ$ at $p_j = 544$ MeV for $m_\pi = 484$ MeV.

I. INTRODUCTION

The scattering of two pions at low energies is the simplest of all dynamical strong-interaction processes from the theoretical standpoint. As pions are the pseudo-Goldstone bosons associated with the spontaneous breaking of chiral symmetry, their low-momentum interactions are constrained by the approximate chiral symmetries of Quantum Chromodynamics (QCD), and the scattering lengths for $\pi\pi$ in the s-wave are uniquely predicted at leading order in chiral perturbation theory (χ PT). Higher orders in the chiral expansion give contributions to these scattering lengths that are suppressed by powers of $(m_\pi/\Lambda_\chi)^2$, where m_π is the mass of the pion, and $\Lambda_\chi \approx 1$ GeV is the scale of chiral symmetry breaking. However, part of these higher-order contributions are from local counterterms with coefficients that are not constrained by chiral symmetry alone. Lattice QCD is the only known technique with which one can rigorously calculate these strong-interaction quantities. A lattice calculation of the $\pi\pi$ scattering length as a function of the light-quark masses, m_q , will allow the determination of the relevant counterterms that appear in the chiral Lagrangian. Of course, this is only true for values of m_q within the chiral regime where $m_q \ll \Lambda_\chi$. Even though it is likely that in the future lattice calculations will be performed at the physical values of the light-quark masses, and while a chiral extrapolation of observables will not be necessary, the values of the counterterms will be essential as the chiral Lagrangian will still be used to compute more-complex strong-interaction processes that are too costly to compute directly on the lattice. A second important motivation for studying $\pi\pi$ scattering with lattice QCD is its impact upon weak-interaction processes (and physics beyond the Standard Model), such as $K \rightarrow \pi\pi$, and the determination of fundamental constants of nature associated with electroweak physics, such as CP violation in the Standard Model.

Lattice QCD calculations are performed on a Euclidean lattice, and the Maiani-Testa theorem demonstrates that S-matrix elements cannot be determined from n-point Green's functions computed on the lattice at finite volume, except at kinematic thresholds [1]. However, Luscher has shown that by computing the energy levels of two-particle states in the finite-volume lattice, the $\pi\pi \rightarrow \pi\pi$ scattering amplitude can be recovered [2]. The energy levels of the two interacting particles are found to deviate from those of two non-interacting particles by an amount that depends on the scattering amplitude and varies inversely with the lattice spatial volume. A number of lattice QCD calculations of $\pi\pi$ scattering in the $I = 2$ channel have been performed previously using Luscher's method. For obvious reasons, calculations were initially performed in quenched QCD [3, 4, 5, 6, 7, 8, 9, 10, 11, 12, 13, 14, 15, 16, 17, 18, 19, 20, 21] but in a recent tour-de-force study, the CP-PACS collaboration exploited the finite-volume strategy to study $I = 2$, s-wave $\pi\pi$ scattering in fully-dynamical lattice QCD with two flavors of improved Wilson fermions [22], with pion masses in the range $m_\pi \approx 0.5 - 1.1$ GeV.

A lattice QCD calculation of $\pi\pi$ scattering should fulfill several conditions: (i) quark masses small enough to lie within the chiral regime so that the extrapolation to the physical point is reliable, (ii) a lattice volume large enough to avoid finite-volume effects from pions "going around the world" but small enough for the energy shifts to be measurable and (iii) a lattice spacing small enough so that discretization effects are under control. Based on these requirements we have performed a fully-dynamical lattice QCD calculation with two degenerate light quarks and a strange quark (2+1) with pion masses in the chiral regime, $m_\pi \approx 294$ MeV (319 configurations), 348 MeV (649 configurations) and 484 MeV (453 configurations). The configurations we have used are the publicly-available MILC lattices

with dynamical staggered fermions of spatial dimension $L = 2.5$ fm, and we have used domain-wall [23, 24, 25, 26] propagators generated by LHPC¹ at the Thomas Jefferson National Laboratory (JLab).

This paper is organized as follows. In Section II we discuss Luscher's finite-volume method for extracting hadron-hadron scattering parameters from energy levels calculated on the lattice. In Section III we describe the details of our mixed-action lattice QCD calculation. We also discuss the relevant correlation functions and outline our fitting procedures. In Section IV we present the results of our lattice calculation, and the analysis of the lattice data with χ^2 -PT. In Section V we conclude.

II. FINITE-VOLUME CALCULATION OF SCATTERING AMPLITUDES

The s-wave scattering amplitude for two particles below inelastic thresholds can be determined using Luscher's method [2], which entails a measurement of one or more energy levels of the two-particle system in a finite volume. For two particles of identical mass, m , in an s-wave, with zero total three momentum, and in a finite volume, the difference between the energy levels and those of two non-interacting particles can be related to the inverse scattering amplitude via the eigenvalue equation [2]

$$p \cot \delta(p) = \frac{1}{L} S \left(\frac{p^2 L^2}{4} \right); \quad (1)$$

where $\delta(p)$ is the elastic-scattering phase shift, and the regulated three-dimensional sum is

$$S(\lambda) = \sum_{\vec{j}} \frac{1}{\vec{j}^2 - \lambda}; \quad (2)$$

The sum in eq. (2) is over all triplets of integers j such that $|\vec{j}| < \infty$ and the limit $\lambda \rightarrow 1$ is implicit [27]. This definition is equivalent to the analytic continuation of zeta-functions presented by Luscher [2]. In eq. (1), L is the length of the spatial dimension in a cubically-symmetric lattice. The energy eigenvalue E_n and its deviation from twice the rest mass of the particle, $E_n - 2m$, are related to the center-of-mass momentum p_n , a solution of eq. (1), by

$$E_n - 2m = 2 \sqrt{p_n^2 + m^2} - 2m; \quad (3)$$

In the absence of interactions between the particles, $p \cot \delta = 1$, and the energy levels occur at momenta $p = 2\pi \vec{j}/L$, corresponding to single-particle modes in a cubic cavity. Expanding eq. (1) about zero momenta, $p \rightarrow 0$, one obtains the familiar relation²

$$E_0 = \frac{4\pi^2}{m L^3} \left[1 + c_1 \frac{a}{L} + c_2 \frac{a^2}{L^2} + O\left(\frac{1}{L^6}\right) \right]; \quad (4)$$

¹ We thank the MILC and LHP collaborations for very kindly allowing us to use their gauge configurations and light-quark propagators for this project.

² We have chosen to use the "particle physics" definition of the scattering length, as opposed to the "nuclear physics" definition, which is opposite in sign.

with

$$c_1 = \frac{1}{\sqrt{4}} \frac{1}{\sqrt{4}} = 0.25 ; \quad c_2 = \frac{1}{\sqrt{2}} \frac{1}{\sqrt{4}} = 0.3535 ; \quad (5)$$

and a is the scattering length, defined by

$$a = \lim_{p \rightarrow 0} \frac{\tan^{-1}(p)}{p} ; \quad (6)$$

For the $I = 2$ scattering length, a_2 , that we consider in this work, the difference between the exact solution to eq. (1) and the approximate solution in eq. (4) is much less than 1%. However, in determining the phase-shift associated with the first excited state on the lattice, the full eigenvalue equation in eq. (1) is solved.

III. DETAILS OF THE CALCULATION

A. Lattices, Actions and Propagators

Our computation of the $I = 2$ scattering amplitude consists of a hybrid lattice QCD calculation using staggered sea quarks and domain-wall valence quarks [28, 29, 30, 31]³. The parameters of the three sets of $N_f = 2 + 1$ asqtad-improved [34, 35] MILC configurations generated with staggered sea quarks [36] that we used in our calculations are shown in Table I. In the generation of the MILC configurations, the strange-quark mass was fixed near its physical value, $am_s = 0.050$, (where b is the lattice spacing) determined by the mass of hadrons containing strange quarks. The two light quarks in the three sets of configurations are degenerate, with masses $am_1 = 0.007; 0.010$ and 0.020 . These lattices were HYP-blocked [37, 38] in order to avoid large residual chiral symmetry breaking. We used the domain-wall valence propagators that had been previously generated by the LHP collaboration on each of these sets of lattices. The domain-wall height is $m = 1.7$ and extent of the extra dimension is $L_5 = 16$. As this is a mixed-action calculation, the parameters used to generate the light-quark propagators have been "matched" to those used to generate the MILC configurations. This was achieved by requiring that the mass of the pion computed with the domain-wall propagators be equal (to few-percent precision) to that of the lightest staggered pion computed from staggered propagators generated with the same parameters as the given gauge configuration [36]. The parameters used in the generation of the domain-wall propagators are shown in Table I. A Dirichlet boundary condition at

TABLE I: The parameters of the MILC gauge configurations and LHPC domain-wall propagators used in our calculations. For each propagator the extent of the fifth dimension is $L_5 = 16$.

Config Set	Dimensions	am_1	am_s	am_{dwf}	$10^3 am_{res}$	# configs	
MILC_2064x21b679m007m050	$20^3 \times 64$	0.007	0.05	0.0081	1.604	0.038	319
MILC_2064x21b679m010m050	$20^3 \times 64$	0.010	0.05	0.0138	1.552	0.027	649
MILC_2064x21b679m020m050	$20^3 \times 64$	0.020	0.05	0.0313	1.239	0.028	453

³ Technical aspects of hybridization are discussed in Ref. [32] and [33].

the midpoint of the time direction ($t = 32$) has been used in generating the LHPC propagators in order to reduce the cost of nucleon matrix-element calculations without affecting their accuracy⁴. Unfortunately, this is not the case for light-pseudoscalar mesons where the signal is sustained for longer time intervals, and hence both the systematic errors and the statistical errors can be improved using correlators of longer time extent.

B. Correlators, Projections and Fitting Methods

In order to perform our calculations of the $\pi\pi$ correlation functions we used the programs Chroma and QDP++ written at JLab under the auspices of SciDAC [39]. In this programming environment, a few lines of C++ code were required to construct the two distinct propagator contractions that contribute to $\pi\pi$ interactions in the $I = 2$ channel. As it is the difference in the energy between two interacting pions and two non-interacting pions that provides the scattering amplitude, we computed both the one-pion correlation function, $C^+(t)$, and the two-pion correlation function $C^{++}(p;t)$, where t denotes the number of time-slices between the hadronic-sink and the hadronic-source, and p denotes the magnitude of the (equal and opposite) momentum of each pion.

The single-pion correlation function is

$$C^+(t) = \sum_x h^+(t;x) \langle \psi^+(0;0) \psi^+(0;0) \rangle; \quad (7)$$

where the summation over x corresponds to summing over all the spatial lattice sites, thereby projecting onto the momentum $p = 0$ state. A $\pi\pi$ correlation function that projects onto the s-wave state in the continuum limit is

$$C^{++}(p;t) = \sum_{\mathbf{p} \neq \mathbf{p}'} \sum_{\mathbf{x} \neq \mathbf{y}} e^{i\mathbf{p} \cdot (\mathbf{x} - \mathbf{y})} h^+(t;x) h^+(t;y) \langle \psi^+(0;0) \psi^+(0;0) \rangle; \quad (8)$$

where, in eqs. (7) and (8), $\psi^+(t;x) = u(t;x) \gamma_5 d(t;x)$ is an interpolating field for the π^+ .

Steps were taken to optimize the overlap between the interpolating fields and the one- and two-pion hadronic states. First, the propagators calculated by LHPC, which all have sources centered about $\mathbf{x} = 0$, were smeared [31, 40] in the neighborhood of $\mathbf{x} = 0$ to maximize overlap with the single-hadron states. Therefore, in eq. (7) and eq. (8), $\psi^+(0;0)$ denotes an interpolating field constructed from smeared-source light-quark propagators. Second, we projected onto two-pion states that are perturbatively close to the energy eigenstates of interest. The two-pion states with zero total momentum that transform in the A_1 representation of the cubic group are, in general, linear combinations of the non-interacting finite-volume eigenstates,

$$|j^+ \pi^+ \pi^+\rangle = d_0 |j^+ (\mathbf{p} = 0) \pi^+ (\mathbf{p} = 0)\rangle + d_1 \sum_{\frac{\mathbf{p}_1}{2} = \mathbf{x} \neq \mathbf{y} \neq \mathbf{z}} |j^+ (\mathbf{p}) \pi^+ (\mathbf{p})\rangle + \dots \quad (9)$$

where d_0 and d_1 are complex coefficients. In the absence of interactions, the ground state is given by the first term in eq. (9), the first excited state by the second term, and so on. In

⁴ Note that the source of each propagator was placed on the $t = 10$ time slice, which led to a maximum of $t = 22$ usable time slices.

the regime $\beta_2 \approx L$, the effect of the interaction is small, as is clear from eq. (4), and each of the terms in eq. (9) are approximate eigenstates. The momentum projection in eq. (8) makes it significantly easier to extract the energies of the interacting eigenstates.

In order to determine the amplitudes and energies of the eigenstates that our correlation functions contain, we used a variety of fitting methods. These include standard covariant fitting, non-covariant fitting, the effective-mass method, singular-value decomposition, single-exponential fits, and multiple-exponential fits. Table II provides a summary of the results of our calculation. For each light quark mass we have chosen to extract the necessary quantities by fitting the correlation functions over the fitting interval given in Table II. Using a covariance-matrix, χ^2 fitting procedure, along with Jackknifing over the lattice configurations, we obtain the central values and statistical errors (the first error quoted for each quantity) shown in Table II. Varying the fitting interval over reasonable ranges provides an estimate of one of the systematic errors associated with the determination of these quantities. The range of central values from a small number of different fitting intervals is used to determine the second error associated with m_π , f_π , $m_\pi = f_\pi$, E_0 , a_2 , m_{a_2} and E_1 , given in Table II. In the calculation of the remaining quantities in Table II, their associated systematic error was estimated by combining statistical and systematic errors of the input quantities in quadrature. For m_π , f_π and β_2 given in units of MeV, there is an additional systematic error arising from the scale setting, which we estimate from the uncertainty in the counterterm, \bar{c}_4 , contributing to f_π , which is discussed subsequently.

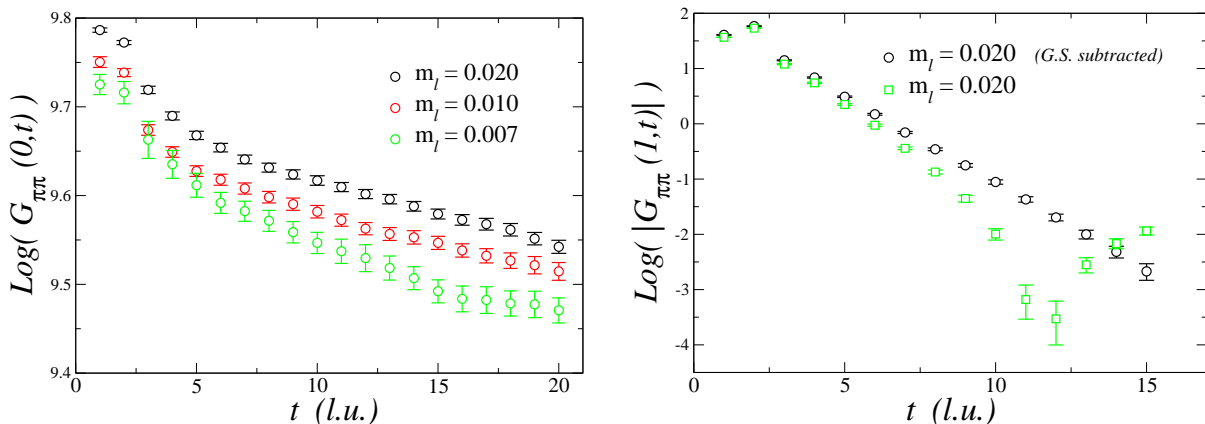


FIG. 1: Log plots of the ratio of correlation functions, $G_{\pi\pi}$, defined in eq. (10). The left panel shows the correlation function $G_{\pi\pi}(0;t)$ for the three sets of MILC configurations, each of which is dominated by the ground-state. The right panel shows the logarithm of the absolute value of $G_{\pi\pi}(2=L;t)$ for the heaviest quark-mass with and without subtraction of the (small) ground-state component.

The pion mass was determined by fitting a single exponential to the pion correlation function, eq. (7). The point-smearing correlator (point-sink and smeared-source) was found to be statistically superior to the smeared-smeared correlator (where the sink is smeared with the same smearing function as the source) both for the one- and two-pion correlators. The

sm eared-sm eared correlator was used only in the determination of the pion decay constant, f_π (see below).

In the relatively large lattice volumes that we are using, the energy difference between the interacting and non-interacting two-pion states is a small fraction of the total energy, which is dominated by the mass of the pions. In order to extract this energy difference we followed Ref. [4] and formed the ratio of correlation functions, $G(p;t)$, where

$$G(p;t) = \frac{C(p;t)}{C(t)^2} \sim \sum_{n=0}^{\infty} A_n e^{-E_n t}; \quad (10)$$

and the arrow becomes an equality in the limit of an infinite number of gauge configurations. In $G(p;t)$, some of the fluctuations that contribute to both the one- and two-pion correlation functions cancel, thereby improving the quality of the extraction of the energy difference beyond what we are able to achieve from an analysis of the individual correlation functions.

In the $p = 0$ case, where we project perturbatively close to the ground state, the correlator $G(0;t)$, shown in Fig. 1, can be fit by a single exponential beyond the first few time slices, and the ground-state energy difference, E_0 , can be determined quite cleanly. For the first excited level, with $p = 2\pi/L$, the momentum projection in eq. (8) eliminates all but approximately 10% (in amplitude) of the ground state contribution, which contributes with opposite sign, as shown in Fig. 1. We analyzed this correlator in two ways. First, by fitting a single exponential to what remains after subtracting the ground-state contribution determined at a distant time slice. Second, by fitting two exponentials, either keeping the value of the ground state energy fixed (three parameter fit) or letting that vary also (four parameter fit). The difference between these procedures, as well as the difference coming from the somewhat arbitrary choice of fitting ranges, is significant only in the value of the two-pion energies and is incorporated in the estimated systematic error. The results of our analysis and the quantities relevant to the determination of the scattering length are summarized in Table II.

IV. ANALYSIS

A main focus of the analysis of lattice data is the extrapolation of the lattice values of various physical and unphysical parameters that hadronic quantities computed on the lattice depend on, in order to make direct comparison with experimental hadronic quantities. Extrapolations in the light-quark masses, the finite lattice spacing and the lattice volume are currently required. For small enough quark masses and lattice spacings, and large enough volumes, one can rigorously perform such extrapolations using low-energy effective field theories. What densities small enough are the dimensionless quantities b_1 , m_1 and m_L . The low-energy effective field theory that can be used to describe the scattering length is χ PT supplemented to include the finite lattice spacing, based on the Symanzik action [41, 42].

Our calculations have generated pions with masses that are less than 500 MeV, which is likely an upper limit to the range of applicability of the chiral expansion. We are confident that the results of the calculations at the lightest two pion masses fall within the chiral regime and can be analyzed with χ PT, while the results of the largest mass point is at the edge of applicability of χ PT.

The effect of the finite lattice spacing is not universal and depends upon the particular discretization used. In our mixed-action calculation, both the sea quarks and valence quarks have been included with actions that have lattice spacing corrections beginning at $O(b^2)$. While $m_{\text{res}} \neq 0$ implies $O(b)$ corrections, these effects are exponentially suppressed with the extent of the fifth dimension and are therefore safely ignored given our current level of precision. In addition, the sea-quark discretization effects are further suppressed by the strong coupling constant β_s since the sea-quark action is perturbatively improved. A generalization of $\overline{\text{PT}}$ suitable to describe this combination of mixed-quark-action discretization has recently appeared in Ref. [43]. Our calculation has been performed at a single value of the lattice spacing and as such we are unable to systematically explore the impact of discretization errors on the determination of the scattering amplitude. In the analysis that follows, we have assumed that the lattice-spacing effects are much smaller than other sources of uncertainty in this calculation, and are neglected⁵.

While the power-law finite-volume dependence of the energy of the two-pion states is used to extract the scattering amplitude using Luscher's method, there are also exponentially suppressed, finite-volume contributions to the observables resulting from pions "going around the world". These corrections are proportional to $e^{-m_\pi L}$ and are further suppressed by a factor $m_\pi^2 = \frac{1}{2}$, since they can arise only from pion loop diagrams. As each of the pion masses that we compute in this work satisfy $m_\pi L \gg 1$, these exponentially-suppressed finite-volume contributions are neglected in the analysis.

A . Scale Setting

In order to determine quantities in physical units, the lattice scale must be traded for a physical scale. In many calculations the mass of the η -meson is used. While this seems fairly convenient, the light-quark mass dependence of the η -meson is controversial (for recent work, see Ref. [46]), and moreover, for light enough pions, the η -meson becomes unstable, and therefore determining its mass in the chiral regime requires a series of calculations of the energy levels of two-pion states in a finite-volume. A short-distance length scale is also commonly used [47], the Sommer scale, r_0 . Such a short-distance scale depends logarithmically upon the light-quark masses, as stressed in Ref. [48], however lattice calculations indicate that the numerical size of the light-quark mass dependence is quite small [49, 50], i.e. the coefficients of unknown operators in the quarkonium chiral lagrangian are numerically small⁶. In this work the pion decay constant, f_π , is used to set the physical length scale. This has the advantage that: (i) f_π is a low-energy parameter with a wellknown dependence on the quark masses (as well as the lattice volume and lattice spacing) determined by $\overline{\text{PT}}$; (ii) the decay constant is easily computed on the lattice with domain-wall valence quarks. We calculate f_π from pion correlation functions via [51]

$$f_\pi = \sqrt{\frac{A_{\text{SP}}}{A_{\text{SS}}}} \frac{2^{\frac{P}{2}} \sqrt{(m_{\text{dw}\pi} + m_{\text{res}})}}{m^{3=2}}; \quad (11)$$

⁵ In the $I = 0$ channel, unlike the $I = 2$ channel, diagrams involving the double pole in the η propagator, proportional to b^2 , lead to modifications to Luscher's formula in eq. (4) that are enhanced by powers of L [44, 45].

⁶ The coefficients are expected to scale as R^{-3} , where R is the characteristic size of the $\overline{Q}Q$ system, from naive dimensional arguments.

where A_{SP} is the amplitude of the one-pion correlation function resulting from a smeared-source and point-sink, and A_{SS} is the amplitude which results from a smeared-source and smeared-sink. The values of m_{dwf} and m_{res} used in this work can be found in Table I.

The chiral expansion of f is [52]

$$f = f_1 + \frac{m^2}{8^2 f^2} \bar{l}_4 + O(m^4); \quad (12)$$

where f is the chiral-limit value of the decay constant, m is the pion mass at leading order in the chiral expansion; $\bar{l}_4 = \log \frac{m^2}{\Lambda^2}$ with Λ an intrinsic scale that is not determined by chiral symmetry. In what follows we will denote the physical values of the various parameters with a phy-superscript. One can use eq. (12) to find

$$\begin{aligned} \frac{m}{f} &= f^{\text{phy}} \left[1 + \frac{1}{4^2} \frac{m^{\text{phy}}}{f^{\text{phy}}} \log \frac{m^{\text{phy}}}{f^{\text{phy}}} \frac{m}{f} \log \frac{m}{f} \right. \\ &\quad \left. + \frac{1}{8^2} \frac{m}{f} \frac{m^{\text{phy}}}{f^{\text{phy}}} \bar{l}_4^{\text{phy}} + O\left(\frac{m^2}{16^2 f^2}\right) \right] \end{aligned} \quad (13)$$

as well as other variants of this formula that differ only by terms of higher order in the chiral expansion. By determining $m = f$ in a lattice calculation, and using the experimental values of m and f (and \bar{l}_4), the pion-decay constant in the lattice calculation at the value of the pion mass, $f(m = f)$, is determined at a given order (in this case next-to-leading order) in the chiral expansion. Higher-order corrections to this scale setting can be determined systematically in the chiral expansion. We use $f^{\text{phy}} = 132 \text{ MeV}$ and $m^{\text{phy}} = 138 \text{ MeV}$. The uncertainty in the scale-independent parameter $\bar{l}_4^{\text{phy}} = 4.4 \pm 0.2$ [52, 53] introduces a source of systematic error of less than 2% in both the pion mass and decay constant. The lattice spacings obtained using this method are given in Table II and may be compared with the determination by MILC [49], $b = 0.1243 \pm 0.0015 \text{ fm}$, using the Sommer scale. The values of the pion masses and decay constants in physical units computed in this paper are consistent with the same quantities computed on the same lattices by MILC in Ref. [49]. For instance, MILC finds $m = 299.99 \pm 0.32 \pm 3.4, 356.46 \pm 0.27 \pm 4.0, 494.27 \pm 0.25 \pm 5.6$ on the 0.007, 0.010 and 0.020 lattices, respectively, where the first error is statistical and the second arises from scale setting. One should keep in mind that (i) results differ at $O(b^2)$ and $O(m^4)$; (ii) the tuning of the domain-wall fermion mass to reproduce the lightest staggered pion mass is done to order 1% accuracy; (iii) Our scale setting procedure includes electromagnetic effects via f^{phy} while MILC's does not.

Rather than using the low-energy constant \bar{l}_4^{phy} as an input to the scale setting procedure, one can perform a two-parameter fit of the lattice data in Table II to the form

$$\begin{aligned} \frac{m}{f^{\text{lu}}} &= b_t f^{\text{phy}} \left[1 + \frac{1}{4^2} \frac{m^{\text{phy}}}{f^{\text{phy}}} \log \frac{m^{\text{phy}}}{f^{\text{phy}}} \frac{m}{f} \log \frac{m}{f} \right. \\ &\quad \left. + \frac{1}{8^2} \frac{m}{f} \frac{m^{\text{phy}}}{f^{\text{phy}}} \bar{l}_4^{\text{phy}} \right] \end{aligned} \quad (14)$$

where f^{lu} is the pion decay constant in lattice units. This procedure gives $b_t = 0.1274 \pm 0.0007 \pm 0.0003 \text{ fm}$ and $\bar{l}_4^{\text{phy}} = 4.412 \pm 0.077 \pm 0.068$ where the first error is

statistical and the second is an estimate of the systematic error. Thus this scale setting procedure is remarkably robust and consistent. One may wonder about the relevance of the chiral logarithm. Repeating the setting procedure with $f^{\text{lat}}: (m = f) = b_t f^{\text{phy}} \sqrt{1 + 1/8^2} (m = f)^2 / m^{\text{phy}} = f^{\text{phy}} / L_t$ yields $b_t = 0.1330 \pm 0.0001$, 0.0001 fm and $L_t = 1.407 \pm 0.010 \pm 0.009$, which are not consistent with MILC scale setting or the experimental value of \bar{l}_4^{phy} , respectively. It would appear that the chiral logarithm is resolved by our data at this order in the chiral expansion.

B. The Scattering Length

With small quark masses and momenta, scattering can be reliably computed in PT . The leading-order result (equivalent to current algebra) was computed in Ref. [54], and the one-loop amplitude was computed in Ref. [52]. While this amplitude is now known at the two-loop level [55, 56], given our current lattice data, we choose to analyze our lattice results at one-loop level. The one-loop expression for the $I = 2$ scattering length is

$$m a_2 = \frac{m^2}{8 f^2} \left[1 + \frac{3m^2}{16^2 f^2} \log \frac{m^2}{2} + l(\mu) \right]; \quad (15)$$

where $l(\mu)$ is a linear combination of scale-dependent low-energy constants that appear in the $O(p^4)$ chiral lagrangian [52] (see Appendix A). We define $l(\mu) = 4 f l$, and therefore we can simply use the ratio $m = f$ computed on the lattice to determine the scattering length using eq. (15). The difference between using the lattice f and a fixed f in the argument of the logarithm modifies the scattering length only at higher orders in the chiral expansion.

The lowest-lying energy eigenvalues in the lattice volume, shown in Table II, allow us to determine the $I = 2$ scattering lengths at the different light-quark masses via eq. (4). Our results for the scattering lengths, and other parameters are presented in the summary table, Table II. The location of the first excited state in the lattice volume allows, in general, for a determination of the phase-shift at non-zero values of the pion momentum via eq. (1). For the lattice parameters in these calculations we were able to extract the $I = 2$ phase-shift at one (large) momentum at the largest quark mass, which is shown in Table II. For the two lighter quark masses, the first excited state is very near the four-pion inelastic threshold, and a simple extraction of the phase-shift is not possible.

The results of our calculation of the product $m a_2$ are shown as a function of $m = f$ in Fig. (2). In addition, we have shown the lowest pion mass datum from the dynamical calculations of the CP-PACS collaboration [22]⁷. The uncertainty in the CP-PACS measurement is significantly smaller than that of our calculation and the agreement is very encouraging. In order to extrapolate $m a_2$ to the physical value of $m = f$, we performed a weighted fit of eq. (15) to the three data points in Table II and extracted a value of the counterterm l . As both quantities, $m a_2$ and $m = f$, are dimensionless there is no systematic uncertainty arising from the scale setting (\bar{l}_4). We determined that $l = 3.3 \pm 0.6 \pm 0.3$, where the first

⁷ We have shown the CP-PACS data point at the lightest pion mass, and at the smallest lattice spacing, $a = 2.10$, and have not attempted to extrapolate their result to the continuum. This lattice spacing is comparable to the one used in this work.

TABLE II: The summary table. The central value for each quantity is determined by fitting the appropriate correlation function over the indicated "Fit Range". The first uncertainty is statistical. The second is an estimate of the systematic error in the fitting process (including varying the fitting range). For quantities with units of MeV, the third uncertainty is theoretical, and is due to the uncertainty in the low-energy constant, \bar{l}_4^{phy} , originating from scale-setting. The chi-square test of fit refers to the extraction of E_0 .

Quantity	$m_1 = 0.007$	$m_1 = 0.010$	$m_1 = 0.020$
Fit Range	6-13	5-15	7-15
m (Lu.)	0.1900 0.0021 0.002	0.2243 0.0010 0.0005	0.3131 0.0012 0.0017
f (Lu.)	0.0937 0.0012 0.001	0.0959 0.0007 0.0002	0.1021 0.0007 0.0012
$m = f$	2.030 0.040 0.03	2.338 0.022 0.005	3.065 0.024 0.030
$\chi^2/\text{d.o.f.}$	0.19	0.84	1.03
E_0 (Lu.)	0.0109 0.0013 0.0003	0.0080 0.0005 0.0003	0.0073 0.0007 0.0004
a_2 (Lu.)	1.12 0.12 0.02	0.99 0.06 0.04	1.22 0.09 0.07
$m a_2$	0.212 0.024 0.004	0.222 0.014 0.009	0.38 0.03 0.02
C	0.29 0.16 0.05	0.021 0.067 0.041	0.017 0.082 0.057
f (MeV)	144.7 0.5 0.4 1.0	148.8 0.3 0.1 1.5	158.0 0.3 0.4 2.8
m (MeV)	293.7 5.9 4.4 2.0	347.9 3.3 0.8 3.4	484.4 3.9 4.9 8.5
b (10^2 fm)	12.78 0.19 0.18 0.09	12.72 0.11 0.09 0.13	12.75 0.13 0.21 0.23
E_1 (Lu.)	0.482 0.070 0.049	0.390 0.030 0.035	0.308 0.009 0.005
$\bar{p}j$ (MeV)	607 44 42 15	551 29 31 12	544 14 12 10
$\langle p \rangle$ (degrees)	{	{	43 10 5

error is statistical and the second is an estimate of the systematic error (see Fig. (2)). This fit of 1 allows, through eq. (15), a prediction of the scattering length at the physical value of the light-quark masses, which we find to be

$$m a_2 = 0.0426 \pm 0.0006 \pm 0.0003 \pm 0.0018 \quad ; \quad (16)$$

The last uncertainty, ± 0.0018 , is the largest and is an estimate of the systematic error resulting from truncation of the chiral expansion of the scattering length⁸. The two-loop expression for the scattering length [53, 56] is given by

$$m a_2 = \frac{m^2}{8 f^2} \left(1 + \frac{3m^2}{16 f^2} \log \frac{m^2}{2} + l^{(1)} \right) + \frac{m^4}{64 f^4} \left(\frac{31}{6} \log^2 \frac{m^2}{2} + l^{(2)} \log \frac{m^2}{2} + l^{(3)} \right) ; \quad (17)$$

where $l^{(2)}$ and $l^{(3)}$ are linear combinations of undetermined constants that appear in the $O(p^4)$ and $O(p^6)$ chiral Lagrangians [52, 56] (see Appendix A). It is not possible to provide

⁸ As a consistency check, one may fit the leading-order χ PT result multiplied by an arbitrary coefficient: $m a_2 = A \frac{m^2}{8 f^2}$. This yields $A = 1.058 \pm 0.059 \pm 0.032$ where the first error is statistical and the second is an estimate of the systematic error. The scattering length at the physical value of the light-quark masses is, in this case, $m a_2 = 0.0462 \pm 0.0026 \pm 0.0014 \pm 0.0018$.

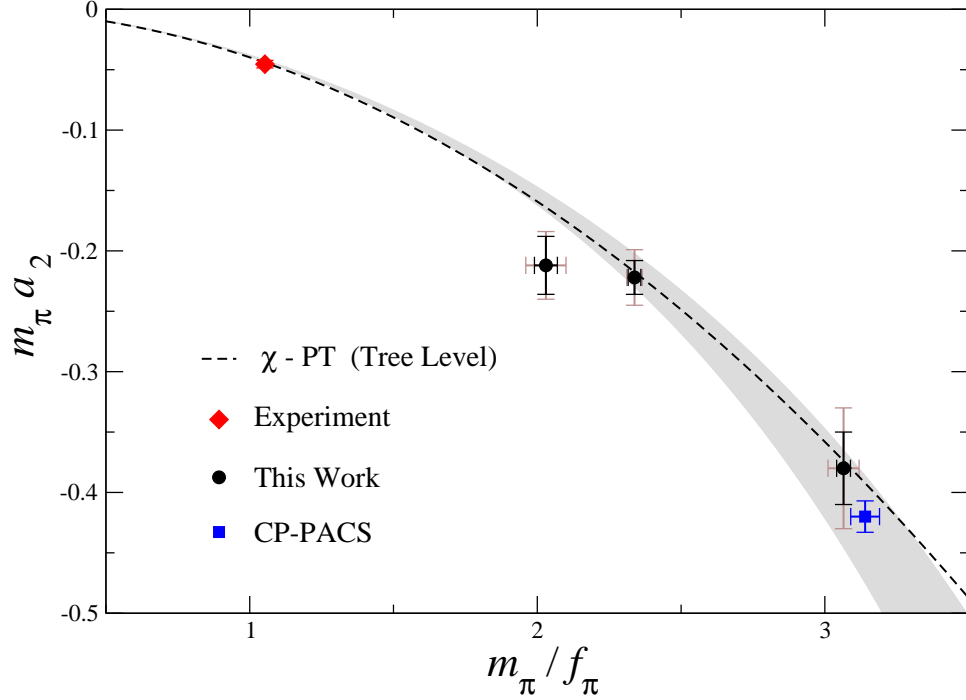


FIG. 2: The results of this lattice QCD calculation of $m_\pi a_2$ as a function of m_π/f_π (ovals) with statistical (dark bars) and systematic (light bars) uncertainties. Also shown are the experimental value from Ref. [57] (diamond) and the lowest quark mass result of the dynamical calculation of CP-PACS [22] (square). The gray band corresponds to a weighted fit to our three data points using the one-loop χ -PT formula in eq. (15) which gives $l_1 = 3.3 \pm 0.6 \pm 0.3$ (the shaded region corresponds only to the statistical error). The dashed line is the tree-level χ -PT result.

a meaningful fit of these three undetermined constants from the few data points we have calculated. While there are estimates of these low-energy constants from a variety of sources, using these estimates in our extrapolation to the physical point would amount to trading one unknown systematic error for another. In order to estimate the systematic error due to extrapolation, we first set $l^{(2)} = l^{(3)} = 0$ and re-fit keeping only the double-log piece at two-loop order. We then set $l^{(3)} = 0$ and do a two-parameter fit to l_1 and $l^{(2)}$. The difference between the extrapolation of the one-loop expression and the extrapolation of the two-loop expression with these simplifications gives the estimate of the systematic error resulting from truncating the chiral expansion.

In Fig. (2) we show the unique prediction of leading order χ -PT for the scattering length (the dashed line), which is seen to agree remarkably well with both the lattice data and the physical value. The gray band in Fig. (2) shows the statistical 1σ region.

In order to better isolate the contributions from higher orders in χ -PT it is convenient to define a scale-independent "curvature" function C :

$$C = \frac{m}{f} \left[1 - \frac{8 f^2 a_2}{m} \right]^{-1} = \frac{3m^2}{16 f^2} \left[\log \frac{m^2}{16 f^2} + 1 \right]^{-1}; \quad (18)$$

where, by construction, $C = 0$ at tree level. The values for $C(m_\pi = f; l)$ that we have calculated are listed in Table II, and are shown in Fig. (3) as a function of $m_\pi = f$ together with the experimental point and the CP-PACS result. A weighted fit of eq. (18) to the

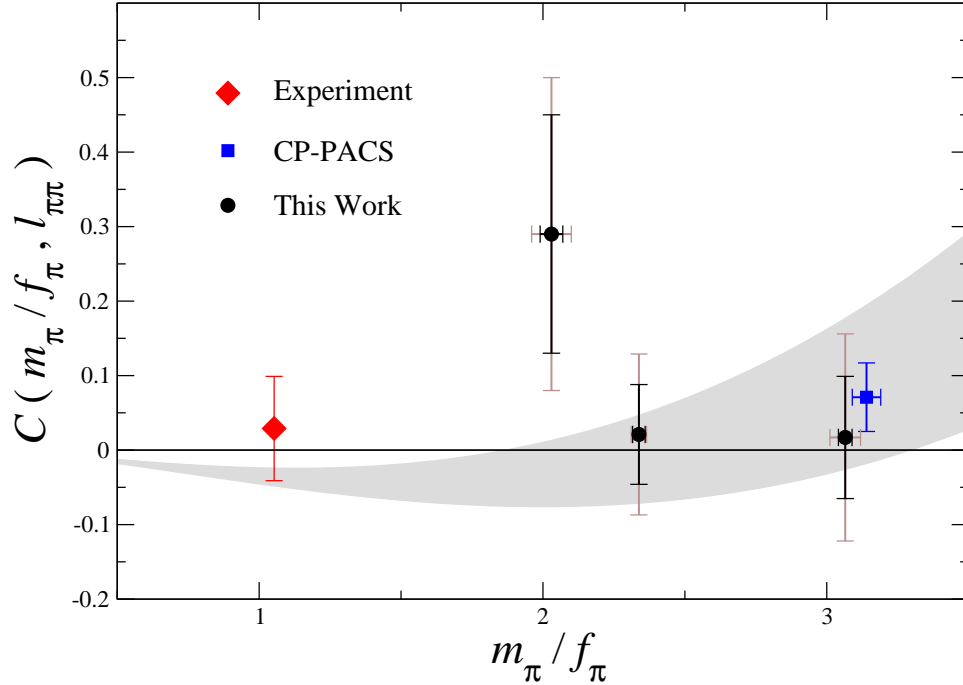


FIG. 3: $C(m_\pi = f; l_{\pi\pi})$ as a function of $m_\pi = f$ for our three lattice data points (ovals) with statistical (dark bars) and systematic (light bars) uncertainties, plotted with the experimental value from Ref. [57] (diamond) and the lowest-mass dynamical CP-PACS [22] point (square). The gray band corresponds to a fit to our three data points (weighted by statistical errors) using the one-loop χ PT formula in eq. (18).

results of the lattice calculation gives: $l = 3.3 \pm 0.6 \pm 0.2$, consistent with the fit to m_{a_2} . The gray band in Fig. (3) shows the 1 σ region for C . The extrapolated value of the scattering length is obviously the same as in the direct fit to m_{a_2} .

The values of l favored by the fits are such that there is an almost perfect cancellation between the counterterm and the logarithm in eq. (15) in the range of m_π considered. This cancellation may be an unfortunate coincidence in this channel. A more refined lattice QCD calculation is required in order to detect the predicted chiral curvature.

The best experimental determination of the $I = 2$ scattering length is obtained through an analysis of $K(e4)$ decays [57], which gives $m_{a_2} = 0.0454 \pm 0.0031 \pm 0.0010 \pm 0.0008$ where the first error is statistical, the second is systematic and the third is theoretical. This data point is plotted in Fig. (2) and in Fig. (3). The two-loop χ PT "prediction" [53] is $m_{a_2} = 0.0444 \pm 0.0010$. Our result is in very good agreement with these determinations.

C . The Phase Shift

We are only able to extract the phase-shift at one non-zero value of the pion momentum, and only at the heaviest pion mass, despite having a relatively clean signal for the first excited state in the lattice volume for all three sets of MILC configurations. The reason for this is that the pion masses are sufficiently light that the first excited state is at an energy very near the four-pion inelastic threshold on the two sets of configurations with the lightest pion masses. At $m_\pi = 484$ MeV, and for pion momentum $|\vec{p}| = 544$ MeV, the phase-shift is found to be $\delta = 43 \pm 10 \pm 5$ degrees.

V . CONCLUSIONS

In this paper we have presented the results of a lattice QCD calculation of the $I = 2$ scattering length performed with domain-wall valence quarks on asqtad-improved MILC configurations with $2+1$ dynamical staggered quarks. The calculations were performed at a single lattice spacing of $b = 0.127$ fm and at a single lattice size of $L = 2.5$ fm with three values of the light quark masses, corresponding to pion masses of $m_\pi = 294, 348,$ and 484 MeV. We have also presented the phase-shift at the heavier quark mass.

We have used one-loop $\overline{\text{PT}}$ to fit the combination of counterterms contributing to scattering at next-to-leading order to the lattice data and extrapolated in the light-quark masses down to the physical point. At the one-loop level we are able to make a prediction for the value of the scattering length, $a_2 = 0.0426 \pm 0.0006 \pm 0.0003 \pm 0.0018$, which agrees within errors with the experimental value.

Acknowledgments

We thank R. Edwards for help with the QDP++/Chroma programming environment [39] with which the calculations discussed here were performed. We are also indebted to the MILC and the LHP collaborations for use of their configurations and propagators, respectively. MJS would like to thank the Center for Theoretical Physics at MIT and the High-Energy and the Nuclear-Theory groups at Caltech for kind hospitality during the completion of this work. The work of MJS is supported in part by the U.S. Dept. of Energy under Grant No. DE-FG 03-97ER 4014. The work of KO is supported in part by the U.S. Dept. of Energy under Grant No. DF-FC 02-94ER 40818. PFB was supported in part by the Director, Office of Energy Research, Office of High Energy and Nuclear Physics, by the Office of Basic Energy Sciences, Division of Nuclear Sciences, of the U.S. Department of Energy under Contract No. DE-AC 03-76SF 00098. The work of SRB is supported in part by the National Science Foundation under grant No. PHY -0400231 and by DOE contract DE-AC 05-84ER 40150, under which the Southeastern Universities Research Association (SURA) operates the Thomas Jefferson National Accelerator Facility.

[1] L. Maiani and M. Testa, Phys. Lett. B 245, 585 (1990).

- [2] K. Huang and C. N. Yang, *Phys. Rev.* 105, 767 (1957); H. W. Hamber, E. Marinari, G. Parisi and C. Rebbi, *Nucl. Phys. B* 225, 475 (1983); M. Luscher, *Commun. Math. Phys.* 105, 153 (1986); M. Luscher, *Nucl. Phys. B* 354, 531 (1991).
- [3] S. R. Sharpe, R. Gupta and G. W. Kilcup, *Nucl. Phys. B* 383, 309 (1992).
- [4] R. Gupta, A. Patel and S. R. Sharpe, *Phys. Rev. D* 48, 388 (1993) [[arXiv:hep-lat/9301016](#)].
- [5] Y. Kuramashi, M. Fukugita, H. Mino, M. Okawa and A. Ukawa, *Phys. Rev. Lett.* 71, 2387 (1993).
- [6] Y. Kuramashi, M. Fukugita, H. Mino, M. Okawa and A. Ukawa, [[arXiv:hep-lat/9312016](#)].
- [7] M. Fukugita, Y. Kuramashi, H. Mino, M. Okawa and A. Ukawa, *Phys. Rev. Lett.* 73, 2176 (1994) [[arXiv:hep-lat/9407012](#)].
- [8] C. Gattringer, D. Hierl and R. Pullirsch [Bem-Graz-Regensburg Collaboration], *Nucl. Phys. Proc. Suppl.* 140, 308 (2005) [[arXiv:hep-lat/0409064](#)].
- [9] M. Fukugita, Y. Kuramashi, M. Okawa, H. Mino and A. Ukawa, *Phys. Rev. D* 52, 3003 (1995) [[arXiv:hep-lat/9501024](#)].
- [10] H. R. Fiebig, K. Rabitsch, H. Markum and A. Mihaly, *Few Body Syst.* 29, 95 (2000) [[arXiv:hep-lat/9906002](#)].
- [11] S. Aoki et al. [JLQCD Collaboration], *Nucl. Phys. Proc. Suppl.* 83, 241 (2000) [[arXiv:hep-lat/9911025](#)].
- [12] C. Liu, J. h. Zhang, Y. Chen and J. P. Ma, [[arXiv:hep-lat/0109010](#)].
- [13] C. Liu, J. h. Zhang, Y. Chen and J. P. Ma, *Nucl. Phys. B* 624, 360 (2002) [[arXiv:hep-lat/0109020](#)].
- [14] S. Aoki et al. [CP-PACS Collaboration], *Nucl. Phys. Proc. Suppl.* 106, 230 (2002) [[arXiv:hep-lat/0110151](#)].
- [15] S. Aoki et al. [JLQCD Collaboration], *Phys. Rev. D* 66, 077501 (2002) [[arXiv:hep-lat/0206011](#)].
- [16] S. Aoki et al. [CP-PACS Collaboration], *Nucl. Phys. Proc. Suppl.* 119, 311 (2003) [[arXiv:hep-lat/0209056](#)].
- [17] S. Aoki et al. [CP-PACS Collaboration], *Phys. Rev. D* 67, 014502 (2003) [[arXiv:hep-lat/0209124](#)].
- [18] K. J. Juge [BGR Collaboration], *Nucl. Phys. Proc. Suppl.* 129, 194 (2004) [[arXiv:hep-lat/0309075](#)].
- [19] N. Ishizuka and T. Yamazaki, *Nucl. Phys. Proc. Suppl.* 129, 233 (2004) [[arXiv:hep-lat/0309168](#)].
- [20] S. Aoki et al. [CP-PACS Collaboration], [[arXiv:hep-lat/0503025](#)].
- [21] S. Aoki et al. [CP-PACS Collaboration], *Nucl. Phys. Proc. Suppl.* 140, 305 (2005) [[arXiv:hep-lat/0409063](#)].
- [22] T. Yamazaki et al. [CP-PACS Collaboration], *Phys. Rev. D* 70, 074513 (2004) [[arXiv:hep-lat/0402025](#)].
- [23] D. B. Kaplan, *Phys. Lett. B* 288, 342 (1992) [[arXiv:hep-lat/9206013](#)].
- [24] Y. Shamir, *Nucl. Phys. B* 406, 90 (1993) [[arXiv:hep-lat/9303005](#)].
- [25] V. Furman and Y. Shamir, *Nucl. Phys. B* 439, 54 (1995) [[arXiv:hep-lat/9405004](#)].
- [26] H. Neuberger, *Phys. Lett. B* 417, 141 (1998) [[arXiv:hep-lat/9707022](#)].
- [27] S. R. Beane, P. F. Bedaque, A. Parreno and M. J. Savage, *Phys. Lett. B* 585, 106 (2004) [[arXiv:hep-lat/0312004](#)].
- [28] W. Schroers et al. [LHPC collaboration], *Nucl. Phys. Proc. Suppl.* 129, 907 (2004) [[arXiv:hep-lat/0309065](#)].

APPENDIX A : THE I = 2 SCATTERING LENGTH AT TWO LOOPS

To accuracy $O(m^6)$ in PT (two loops), the scattering length is given by [56]

$$m a_2 = \frac{m^2}{8 f^2} \left(1 - \frac{m^2}{8^2 f^2} h + 16^2 B^i + \frac{m^4}{64^4 f^4} \left(\frac{262}{9} - \frac{22}{9} + 64^2 B \right) \right) \quad (\text{A1})$$

where

$$\begin{aligned} B = & \frac{3}{32^2} \log \frac{m^2}{2} + 8(l_1 + l_2) + 2(l_3 - l_4) - \frac{3}{32^2} \\ & + 2 \frac{m^2}{f^2} \left(\frac{1}{16^2} (24l_1 + 16l_2 + 15l_3 - 6l_4) + \frac{47}{12} \frac{1}{16^2} \log \frac{m^2}{2} + \frac{1861}{2304^2} \right) \\ & + \frac{31}{6} \frac{1}{16^2} \log \frac{m^2}{2} - \frac{1}{8^2} [l_4 + 2(2l_1 + l_3 + 6l_2)] \log \frac{m^2}{2} \\ & - \frac{5}{4} l_3^2 - 8 l_3^2 + 4 l_4 [8l_1 + 3l_3 + 8l_2] + r_1 + 16r_4 \quad : \quad (\text{A2}) \end{aligned}$$

The l_i and r_i are scale-dependent low-energy constants that appear in the $O(p^4)$ and $O(p^6)$ chiral lagrangians [52, 56], respectively.